Omni-supervised Facial Expression Recognition via Distilled Data

Ping Liu, Yunchao Wei, Zibo Meng, Weihong Deng, Joey Tianyi Zhou, and Yi Yang

Abstract—Facial expression plays an important role in understanding human emotions. Most recently, deep learning based methods have shown promising for facial expression recognition. However, the performance of the current state-of-the-art facial expression recognition (FER) approaches is directly related to the labeled data for training. To solve this issue, prior works employ the pretrain-and-finetune strategy, *i.e.*, utilize a large amount of unlabeled data to pretrain the network and then finetune it by the labeled data. As the labeled data is in a small amount, the final network performance is still restricted. From a different perspective, we propose to perform omni-supervised learning to directly exploit reliable samples in a large amount of unlabeled data for network training. Particularly, a new dataset is firstly constructed using a primitive model trained on a small number of labeled samples to select samples with high confidence scores from a face dataset, *i.e.*, MS-Celeb-1M [1], based on feature-wise similarity. We experimentally verify that the new dataset created in such an omni-supervised manner can significantly improve the generalization ability of the learned FER model. However, as the number of training samples grows, computational cost and training time increase dramatically. To tackle this, we propose to apply a dataset distillation strategy to compress the created dataset into several informative class-wise images, significantly improving the training efficiency. We have conducted extensive experiments on widely used benchmarks, where consistent performance gains can be achieved under various settings using the proposed framework. More importantly, the distilled dataset has shown its capabilities of boosting the performance of FER with negligible additional computational costs. We hope this work will serve as a solid baseline and help ease future research in FER.

Index Terms—Facial Expression Recognition, Omni-supervised Learning, Dataset Distillation.

1 Introduction

As one of the most important emotion and intention sensing cues for human communications, facial activities have been extensively studied in the past decades. A robust facial expression recognition (FER) system should be able to recognize the basic expressions [2], *i.e.*, anger, disgust, fear, happy, sad, surprise, and/or compound expressions from expressive facial images. With the development of deep Convolutional Neural Networks (CNNs) [3], [4], [5], various deep learning models have been designed for facial activity analysis [6], [7], [8], [9], [10], [11], [12].

As a data driven approach, CNNs require a huge amount of labeled data with high quality for training. However, collecting and annotating data with sufficient diversities is time-consuming and laborious. To solve this issue, researchers propose various ways to train deep models with limited data [13], [14], [15]. For example, Santander *et al.* [14] proposed to combine a group of small datasets into a large dataset to improve the performance. However, using such a dataset consisting of heterogeneous data for training requires a carefully designed training strategy, *e.g.*, weights initialization, data augmentation etc to achieve a satisfactory result.

Inspired by semi-supervised learning, researchers have devoted efforts to studying how to take advantage of the huge amounts of unlabeled facial images from Internet for training FER systems, along with the existing datasets with limited labeled samples. One plausible way of making use of those huge-scale unlabeled data, is to utilize them to pretrain a network [16] in an unsupervised [17] or self-supervised [18] manner, and then use the pretrained network to finetuning based on the limited annotated data. However, as the dataset used in the finetuning step is of a small size, the knowledge learned by the network might be quite restricted.

From a different perspective, in this work, we propose a simple yet effective baseline of omni-supervised facial expression recognition. In particular, under the omni-supervised learning setting, we select useful samples from a huge scale unlabeled data in an *automatic* manner. The selected samples is utilized to construct a large dataset, which is combined with existing small scale datasets for training the FER model, rather than for pretraining. Comparing to previous works following the pretraining-finetuning pipeline, our method has more advantages: it directly applies the large amount of samples selected from unlabeled data on network training, learning more abundant knowledge for the target task.

Although the dataset constructed by the above mentioned method can significantly improve the performance of FER, which has been proved in our experiment, it still has issues. First, the size of the constructed dataset can be large (e.g. hundreds of thousands of samples), making the FER learner training process time-consuming. Second, since the constructed dataset is annotated automatically,

P. Liu, Joey Zhou are with Center for Frontier AI Research, Agency for Science, Technology, and Research, Singapore.

Y. Wei is with Institute of information science, Beijing Jiaotong University, Beijing, China.

Y. Yang is with Centre for Artificial Intelligence, University of Technology Sydney, Sydney, Australia.

W. Deng is with Pattern Recognition and Intelligent System Laboratory, Beijing University of Posts and Telecommunications, Beijing, China.

Z. Meng is with InnoPeak Technology Inc., Palo Alto, USA.

there might exist some incorrectly labeled samples. Third, the number of selected samples in each class might not be balanced, which might bring bias for training. To tackle the above-mentioned issues, we propose to utilize the dataset distillation strategy [19] to distill the key knowledge from the constructed large scale dataset. The distilled knowledge is compressed into a small set of images, *e.g.*, in our case, one image represents one single category. Comparing to the original constructed dataset, the computational cost of the distilled images is decreased significantly. Although with a surprisingly small size, the distilled dataset is capable of boosting the recognition accuracy to a higher stage in both inner-dataset evaluation and cross-dataset evaluation comparing to the models trained using only the labeled datasets

In general, we list our main contributions in this work as follows:

- We propose an omni-supervised facial expression recognition baseline method. Specifically, we construct a large-scale dataset and exploit it under the omni-supervised pipeline. Unlike previous works utilizing an unlabeled large-scale dataset to pre-train the network and provide initialization for downstream fine-tuning, our method constructs a largescale dataset from the huge amount of unlabeled data, and utilize the constructed dataset as well as the existing small scale labeled dataset to improve the FER performance.
- To improve the generality, decrease the training cost, and minimize training bias due to class imbalance, we propose to utilize the dataset distillation strategy to summarize the knowledge from the constructed dataset. Specifically, by the dataset distillation strategy, the constructed dataset, which has around 140K images, is compressed into a significantly small image set, in which one image for each class. The highly summarized knowledge in the distilled small set can be exploited together with the small size manually labeled data to improve the generality power of the FER learner.
- We conduct extensive experiments on FER benchmarks, demonstrating the superiority of the simple yet effective baseline method.

2 RELATED WORK

This section will focus on facial expression recognition and semi-supervised learning, which are the most related topics with this article.

2.1 Facial Expression Recognition

With the development of modern convolutional neural networks, various deep learning methods have been applied to facial expression recognition. Recent deep learning based methods [6], [7], [8], [20], [21], [22] outperform their counterparts using traditional machine learning techniques [23], [24], [25], [26], [27], [28], [29], [30], [31], [32], [33], [34], [35], [36], [37]. [20] proposes to unify Deep Belief Network and Boosting methods to perform feature learning, feature selection, and classifier construction in a joint way.

[21] constructs an Inception-wise network and achieves promising recognition rates on seven public facial expression databases. To obtain discriminative features, [6], [7], [8] propose to disentangle expression-sensitive knowledge and analyze the facial expressions based on the expressionsensitive knowledge. To suppress the variations introduced by identities, [6] proposes an identity-aware convotional neural network to differentiate the identity sensitive knowledge from expression sensitive knowledge. [7], [38] propose to utilize generative adversarial networks (GANs) to disentangle expression variations from pose variations. [8] proposes to extract facial expressive information by a designed de-expression module. To recognize facial expressions with occlusions, [22] proposes to utilize attention mechanisms in CNNs and [39] utilizes a privileged learning mechanism to adjust the importance of feature learned from different facial regions. Interested readers can read [40] for a systematic review of deep facial expression recognition works.

2.2 Semi-supervised Learning

A successful CNN based feature learning process is heavily dependent on large scale training data with high-quality labels. Unfortunately, manually labeling huge amounts of data in high quality is time-consuming and labor-expensive. More than that, in FER, due to the privacy concern, labeled data collection itself is also a question. To deal with this limitation, semi-supervised learning [41], [42], [43], [44], [45], [46] is utilized to improve the performance. Among those previous works, [46] follows a strategy that has been proved effective in previous works: introduce huge scale unlabeled data to pretrain the network, providing a good initialization for the downstream finetuning process. However, there are a few issues in this strategy [46]. Introduce huge-scale unlabeled data to pretrain the network occupies additional computation cost. The finetuning step still use a small scale dataset, which restricts the knowledge learned by the network. On the contrary, our method is based on omni-supervised learning, combining a huge-scale dataset, which is constructed automatically from a huge-scale unlabeled dataset, with a small size labeled dataset. By this way, the constructed dataset participates in the FER learner training process, rather than acting as an initializer.

3 METHODOLOGY

In this section, we illustrate the details of the proposed method step by step. As shown in Fig. 1, first, we utilize the manually labeled data in a small size to train a primitive FER learner (Sec. 3.2). Second, this primitive FER learner is then utilized to provide guidance to select the most confident unlabeled data from huge-scale sets (Sec. 3.3). Specifically, unlike previous works choosing the confident samples based on their category likelihood, this proposed baseline method is based on the similarity between highlevel features extracted from the layer before the softmax output layer. Since this primitive FER learner embeds the knowledge from the manually labeled data in itself, the samples selected by it shares the similar statistical characteristics with the manually labeled ones. Consequently, the problem of "domain shift" between the selected samples and the

manually labeled samples can be relieved. Those huge scale selected samples are constructed into a new dataset, which will collaborate with the original small size labeled dataset to strengthen the FER learner directly. Further, to decrease the computation cost, save the training time, and increase the generality of the network, we propose to utilize the dataset distillation strategy [19] to compress the huge-scale constructed dataset into a very small set, in which one image for one class (Sec. 3.4).

3.1 Task Definition

Facial expression recognition aims to learn a mapping function to map the original input image x to a latent representation. This latent representation should have the discriminative capability to distinguish samples from different classes. In this article, the mapping process is conducted by a convolutional neural network (CNN), which is denoted as $f(;\theta)$ and learned by labeled data $\{x_i^l,y_i^l\}, 1\leq i\leq N$. The learning formulation is as follows:

$$min \sum_{i=1}^{N} \sum_{j=1}^{m} \mathcal{L}(\mathbf{w}_{j}^{T} \cdot f(x_{i}; \theta), y_{i})$$
 (1)

where $\mathcal{L}(,)$ is a cross-entropy loss function, \mathbf{w}_j is the classifier parameter for j-th class, θ is the CNN parameter, \mathbf{m} is the class number.

We target to improve the generality of the learned network $f(;\theta)$ by constructing a large scale dataset and apply it under the omni-supervised learning setting, which will be discussed in the next subsections.

3.2 Primitive Learner Training on Labeled Data

As shown in Figure. 1(a), in the first step, we utilize an existing small scale labeled dataset, denoted as $\{x_i^l, y_i^l\}$, to train a primitive learner $f(;\theta)$. To make the following discussion convenient, we name the utilized labeled dataset in this step as the anchor data. Given the anchor data, the primitive learner is trained by optimizing Eq. 1 via stochastic gradient descent [47].

3.3 Auxiliary Samples Selection from Unlabeled Data

This subsection illustrates how to select reliable samples from a huge scale unlabeled dataset, which is denoted as $\{x_i^{ul},y_i^{ul}\}$. To make the FER learner benefit from the selected unlabeled samples, the selected data should share similar statistical distributions with the labeled ones. Concretely, for each unlabelled data x_i^{ul} , we feed it to the primitive learner $f(;\theta)$ to generate its latent features $f(x_i^{ul};\theta)$ and corresponding class confidence score by the following formulation:

$$P(y_i|f(x_i^{ul};\theta)) = \frac{\exp(\mathbf{w}_i^T \cdot f(x_i^{ul};\theta))}{\sum_{j=1}^m \exp(\mathbf{w}_j^T \cdot f(x_i^{ul};\theta))},$$
 (2)

where \mathbf{w}_j is the weight vector for the j-th class, m is the number of classes.

How to choose the appropriate samples sharing similar statistical distribution with the manually labeled data? One possible way is to utilize the probability score for

the selection. Utilizing unlabeled data with pseudo labels generated by probability scores to update the learner has been explored in previous works on semi-supervised learning [41] and unsupervised learning [48]. However, in FER, the labeled data and unlabeled data are usually collected in different environments, making the conditional distributions between those databases different. As pointed out by [16], in such cases, the generated probability scores and corresponding pseudo labels, might be error-prone.

To deal this issue, we utilize the same strategy in [49]: we generate pseudo labels for the unlabeled data based on the semantic feature similarity. As pointed out in [49], for samples x_* in the same class, the corresponding learned latent features $f(x_*;\theta)$ have a tendency to cluster together. The dimension of $f(x_*^{ul};\theta)$ is usually much higher than that of probability score vector $P(y_*|x_*^{ul})$, making them more robust in learning processes.

Following the the strategy mentioned above, we feed each labeled sample x_i^l into the primitive network $f(;\theta)$ to calculate its latent feature representation $f(x_i^l;\theta)$. Since we have the ground truth for those labeled data, we can calculate the centroid in the feature space for each class by the following formulation:

$$center_k = \frac{\sum_i \mathbb{1}(y_i^l = k) \cdot f(x_i^l; \theta)}{\sum_i \mathbb{1}(y_i^l = k)},$$
 (3)

where $\mathbb{1}()$ is the indicator function, k is the class index.

As shown in Figure. 1(b) and (c), for each unlabeled data sample x_i^{ul} , we feed it into the primitive FER learner to produce its feature representation $f(x_i^{ul};\theta)$, and then compute the cosine distance between $f(x_i^{ul};\theta)$ and each class centroid $center_k$:

$$d(center_k, f(x_i^{ul}; \theta)) = cos(center_k, f(x_i^{ul}; \theta))$$
 (4)

Then, we set the pseudo label for each unlabeled sample \boldsymbol{x}_i^{ul} based on the following criterion:

$$y_i^{ul} = \hat{k}, If \ d(center_{\hat{k}}, f_i) \le d(center_k, f_i) - \delta, \forall k \ne \hat{k}$$
 (5)

where k is the class index for the facial expressions, δ is a margin threshold.

The samples selected from the unlabeled dataset based on the above criterion would share the similar statistical distribution with the labeled samples. They collaborate with the existing small scale labeled data to construct a large scale dataset, which is utilized to refine the primitive FER learner $f(;\theta)$. To make the following discussion simple, we name those selected samples from an unlabeled database by our method as auxiliary samples. In our experiment, the number of auxiliary samples selected from the unlabeled MS1M-Celeb-1M (MS1M for short) is 137, 769. We show examples of selected auxiliary samples in Figure. 3, in which selected samples are sorted by their cosine distance values to the nearest class centroid.

The efficacy of the auxiliary samples selected from the huge-scale unlabeled dataset are demonstrated in our experimental results, which will be discussed in Sec. 4.4.1 and 4.4.2.

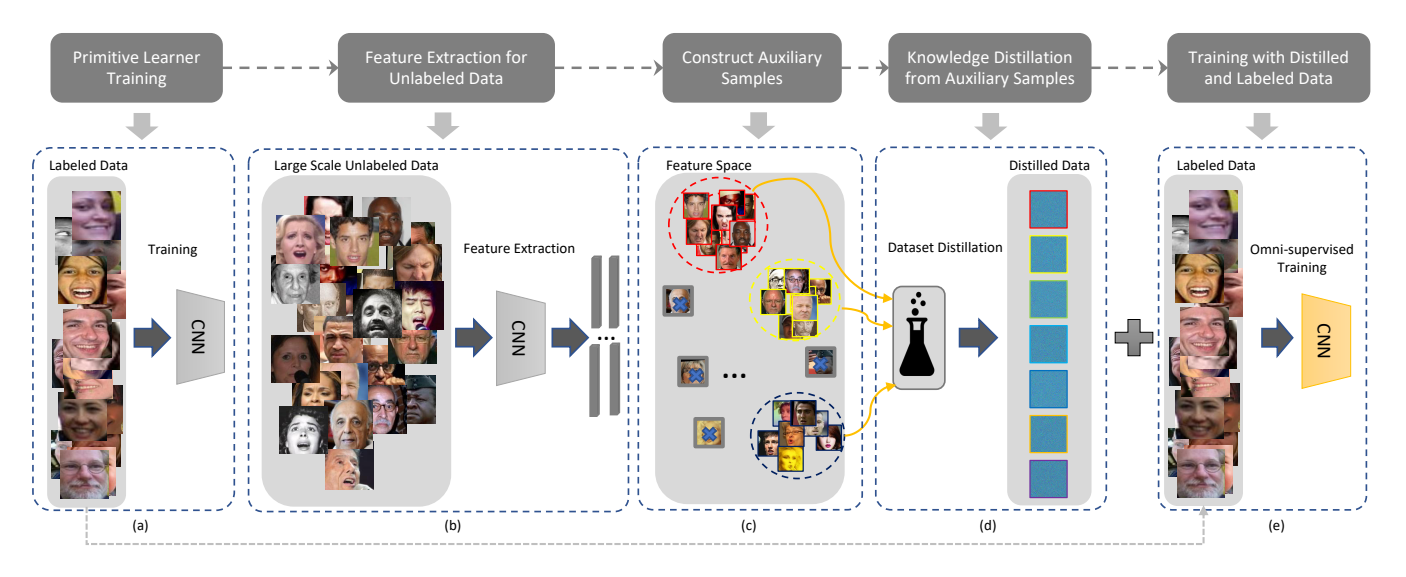


Fig. 1. An illustration for the whole pipeline. First, we utilize labeled data on hand to train a primitive classifier. Since the labeled dataset for FER is often with a small size, the computation cost in this step is not huge and acceptable. Second, this primitive classifier will be utilized to provide guidance to select the most related unlabeled data from large-scale sets. Specifically, unlike previous works choosing the related samples based on their category likelihood, this proposed baseline method is based on high-level features with semantic meaning, which is extracted by the utilized primitive classifier. Knowledge related to FER will be injected into the training process, in which the useful information from unlabelled data and labeled data both contribute to the network training. Since the unlabelled data set probably consists of huge amounts of data, we utilize dataset distillation strategy [19] to compress the knowledge into a highly refined set, i.e., one image for each class in our case. This highly distilled knowledge from huge-scale unlabeled data will be combined with the original labeled data together to train a stronger FER learner.

Algorithm 1 Dataset Distillation Process

Input: the selected auxiliary samples with size N; n: the distilled sample number; $p(\theta)$: distribution of initial network weights; η_0 : initialization for η ; α : step size; M: batch size; T: the iteration number;

```
1: Initialize: \tilde{\mathbf{x}} = {\{\tilde{x}_i\}_{i=1}^n, \eta = \eta_0}
  2: for t = 1; t \le T; t + + do
              fetch the current batch data \mathbf{x}_t = \{x_{t,j}\}_{j=1}^M
  3:
              sample a batch of initial weights \theta_0^j based on distri-
  4:
       bution p(\theta_0)
              \mathbf{for} \ \mathrm{each} \ \mathrm{sampled} \ \theta_0^j \ \mathbf{do}
  5:
                    \theta_1^j = \theta_0^j - \eta \nabla_{\theta_0^j} \check{l}(\tilde{\mathbf{x}}, \theta_0^j)
  6:
  7:
  8:
              Update: \tilde{\mathbf{x}} = \tilde{\mathbf{x}} - \alpha \nabla_{\tilde{\mathbf{x}}} \sum_{j} L^{j}, \eta = \eta - \alpha \nabla_{\eta} \sum_{j} L^{j}
10: end for
Output: distilled data \tilde{\mathbf{x}}
```

3.4 Knowledge Distillation from Auxiliary Samples

Although the selected auxiliary samples can be used to boost the FER model performance, their large size brings significant computation cost ¹. Other than that, it is inevitable that some noisy samples still exist in those selected data. To minimize the computation cost and negative impact from noisy auxiliary samples, we deploy dataset distillation [19]. Unlike model distillation, which distills knowledge from a set of separately trained learners into a compact one, dataset distillation conducts an orthogonal task: keep the learner fixed while distill the knowledge existing in a whole dataset and compress them into a sparse set of synthetic images. By an elegantly designed algorithm [19],

1. The size might keep increasing if we utilize more unlabeled data collected from the internet.

the distilled image set, although with a small size, has the capability to achieve the same or comparable performance.

Assume we have selected N auxiliary samples, the target in this step is that we would like to encapsulate the knowledge in those N samples into n distilled samples, where $n \ll N$. Following [19], we perform the dataset distillation process as detailed in Alg. 1, by which we distill the knowledge from the huge size of auxiliary samples into a small set of synthetic images, denoted as $\tilde{\mathbf{x}}$. We utilize the distilled $\tilde{\mathbf{x}}$ as well as the existing small scale dataset, *i.e.*, $\{x_i^l\}$, to refine our FER learner.

In summary, utilize the distilled auxiliary samples rather than the vanilla auxiliary samples has a few advantages: 1) the distilled images are with a small size, introducing few computation cost; 2) comparing to the vanilla auxiliary collected samples, the distilled images are with high generality capability, which has been experimentally proved to benefit to the cross-dataset evaluation settings.

4 EXPERIMENTAL RESULTS

In this section, we evaluate our method on benchmark datasets. The details about evaluation settings, datasets, implementation details, and performance comparisons are discussed in the following subsections.

4.1 Evaluation Settings

We employ two evaluation settings, *i.e.*, inner-database evaluation, and cross-database evaluation. In Inner-database evaluation, the training set and test set are from the same database. For example, if we conduct an inner-evaluation on RAF-DB 2.0, we use RAF-DB 2.0 training set and constructed dataset to train an FER learner, and then use the trained learner for evaluating the RAF-DB 2.0 test set. In Cross-dataset evaluation, the training set and test set are from different databases.

4.2 Databases

Experiments are conducted on five datasets, including Real-world Affective Face Database (RAF-DB) 2.0 [50], FER-2013 [51], Extended CohnKanade (CK+) [2], Japanese Female Facial Expression (JAFFE) [52], and MMI [53]. Auxiliary samples are selected from MS1M [1], which does not have any expression labels and therefore is considered as an unlabeled database.

RAF-DB 2.0 [50] contains 29,672 facial images which are collected from the Internet. It is a real-world database consisting of highly diverse samples. To achieve reliable labels for those samples, manually crowd-sourced annotation is conducted in [50]. There are two emotion sets in this dataset, *i.e.*, the basic expression label set, and the compound emotion label set. In this article, we focus on recognizing the basic expressions, and therefore we only utilize the basic expression label set, where there are 15,339 images divided into a training set (12,271 images) and a test set (3,068 images). To save the space, we use RAF-DB to denote RAF-DB 2.0 dataset in our discussion.

FER-2013 [51] was constructed for the ICML 2013 Challenges in Representation Learning, which contains 28,709 training images, 3,589 validation images, and 3,589 test images with basic expression labels. After being collected from the Internet automatically by Google search engine, all images are aligned and resized to 48×48 pixels.

CK+ [2] is a laboratory-controlled database that has been widely used in previous works for FER, where there are 593 video sequences collected from 123 subjects. In each sequence, there is a shift from a neutral expression in the first frame to the peak expression in the last frame. Among the 593 video sequences, there are 327 sequences labeled with basic expressions based on the Facial Action Coding System (FACS). Since CK+ does not provide official training/validation/test sets split, to make a fair comparison, we follow the setting in the previous work [20] to prepare the data. Specifically, first, we utilize the first frame as the neutral face of each labeled sequence and the last three peak frames with corresponding labels, resulting 1,308 images in total. Then the 1,308 images are divided into 10 groups for n-fold cross-validation experiments.

MMI [53] is constructed in a lab controlled environment, where there are 326 sequences in total, among which 213 sequences have basic expressions labels. Different from CK+, MMI is onset-apex-offset labeled, where the sequence in MMI begins with a neutral expression, reaches the peak expression in the middle, and then returns to a neutral expression. Pointed out by [40], the subjects in MMI might perform the same expression in different ways, and occlusions, *e.g.*, glasses, mustache, exist in some of the subjects.

JAFFE [52] is a laboratory-controlled database containing 213 samples from 10 Japanese females, where each subject performs basic expressions 3 or 4 times. Due to the limited number of samples in this database, we utilize a leave-one-subject-out experimental setting.

MS-Celeb-1M(MS1M) [1] is a benchmark for the celebrity recognition. All images in MS1M are collected from the Internet. In version 1 of this dataset, there are around ten million images of one million celebrities captured in real scenarios. Due to its huge scale and variations, MS1M becomes

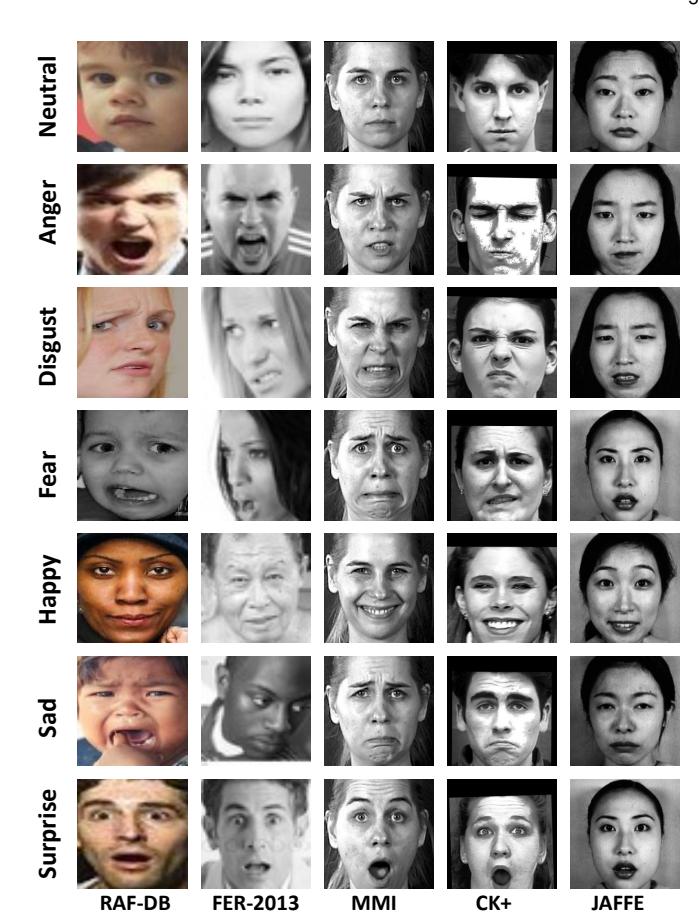


Fig. 2. Visualizing examples from utilized databases. From top to bottom: neutral, anger, disgust, fear, happy, sad, and surprise. From left to right: RAF-DB 2.0, FER-2013, MMI, CK+, and JAFFE. Best viewed in color.

one of the most challenging datasets for face recognition and face verification. There are 85,742 identities with 5,822,653 images in this pre-processed version, in which all the images are aligned by MTCNN [54] and resized to 112×112 . There is no expression label in this database, and therefore we treat it as an unlabeled database in this work.

In Figure. 2, we show some example images from the databases utilized in this article. Those databases are collected in different scenarios, and therefore they have their own data bias. For example, 1) all faces in CK+ and JAFFE are frontal, while in RAF-DB, FER-2013, large face pose variations exist; 2) in FER-2013, CK+, and JAFFE, there is little color information to utilize; 3) the way to express "anger" in RAF-DB, FER-2013 are quite different from that in CK+ and JAFFE. We choose RAF-DB as the anchor database to select samples from MS1M, and use the selected samples to construct an auxiliary database for FER.

4.3 Implementation Details

In our experiments, we utilize two different architectures, *i.e.*, VGG-Face [55] and ResNet-34 [56], to test the efficiency and generality of our method. We choose those two architectures since they are the most frequently used networks in recent FER works [6], [46].

All the images utilized in our experiments are aligned by MTCNN [54] and resized to 224×224 . A data augmentation strategy of randomly horizontal flipping with 50% probability is utilized. During training, we utilize stochastic gradient

descent with 0.9 momentum to optimize the network. The initial learning rate is set to 0.001, which will be multiplied by 0.1 every ten epochs. Unless noted, the total epoch number is set to 25. We implement the experiments by PyTorch [57] and run all settings on a workstation with four NVIDIA GTX 2080Ti GPU cards.

4.4 Performance Evaluation

This section verifies the efficacy of our method in both discriminative ability and generality capability. We conduct inner-database evaluation at first and cross-dataset evaluation at second. The performance is evaluated by the mean classification accuracy.

4.4.1 Inner-dataset Evaluations

We conduct the inner-dataset evaluations on two in-the-wild databases, *i.e.*, RAF-DB, FER-2013 and one lab-controlled database, *i.e.*, CK+. We report comparisons with the prior works under the similar settings in Table.1, 2, and 3. In the experiment, RAF-DB is utilized as the anchor dataset for training the primitive learner. Auxiliary samples are selected from MS1M. To save the space, the auxiliary samples after data distillation are denoted as DAS (Distilled Auxiliary Samples), while the auxiliary samples before distillation are denoted as VAS (Vanilla Auxiliary Samples).

In Table. 1, we report our performance on RAF-DB. Based on Table. 1, we can find that by utilizing the auxiliary samples selected from MS1M, the proposed method outperforms the previous works. Specifically, compared to the previous work utilizing new loss functions [58], our method does not need any new loss functions. Comparing to [46] introducing more human labels into training, our method still outperforms it by almost 2% with few label cost. Since DAS is with a smaller size, its computation cost is much lower than VAS. The computation cost comparison is shown in Table. 8. Comparing to the performance of VAS, the performance of DAS is still comparable, which is 86.55% vs. 85.84% on VGG-Face, 85.24% vs. 85.84% on ResNet-34, respectively. Considering the much less data size, the distilled data achieves a good balance between computation cost and final performance.

Table. 2 shows results comparison on FER-2013. On this challenging dataset, we find that the constructed dataset by our omni-supervised learning strategy and the distilled data both outperformed previous works under a similar setting. For example, comparing to the baseline with VGG-Face backbone, introducing the constructed dataset in an omnisupervised manner achieves a higher prediction accuracy; more than that, the distilled data boosts the performance to a higher stage by distilled key knowledge and keeping a sample balance from the constructed data.

From Table. 1 and 2, we can find that: 1) VGG-Face network has better results than ResNet-34. We believe this is because VGG-Face is pretrained on a face recognition dataset while ResNet-34 is initialized on ImageNet, which makes VGG-Face more suitable to face tasks. 2) distilled auxiliary samples achieve the best recognition accuracy in both settings, *i.e.* 86.55% on RAF-DB and 73.27% on FER-2013, which demonstrates that the distilled images contain key knowledge benefiting to the FER learner.

For CK+, we only conduct the experiment using VGG-Face and report the performance in Table. 3. Since the data size of CK+ is much smaller than the size of vanilla auxiliary data, we do not conduct the experiment on CK+ with vanilla auxiliary samples, but only report the accuracy using distilled auxiliary samples. In Table. 3, we can find that our method performs better than the baseline [46] and [21], or achieves comparable accuracy to [46]. But unlike [46], our method is with much less label cost.

4.4.2 Cross-dataset Evaluations

The cross-dataset evaluations and comparisons with previous state-of-the-arts are shown in Table. 4-7. Four datasets are used for test, which include: CK+, JAFFE, MMI, and FER-2013. We make a comparison with [16], which has the latest results on cross-dataset evaluation settings. Following the setting as [16], we use the combination of RAF-DB and distilled auxiliary samples selected from MS1M as training set. In this work, we do not compare to the prior methods utilizing specifically designed domain adaptation strategies due to two reasons: 1) our research focus is to demonstrate the efficacy of our omni-supervised FER method and the distilled data; 2) the domain adaptation strategies proposed in prior works for minimizing the domain gap between different datasets, such as [59], [60], [61], [62], are complementary to our work and can collaborate together.

Based on experimental results in Table. 4-7, we can find that our method outperforms or achieves comparable results. We will give a more detailed analysis of the results for each dataset in the following paragraphs.

As shown in the Table. 4, our method achieves better performance than [16]. Unlike [16] using explicit domain adaptation strategy to minimize the domain gap between source dataset and target dataset, the better performance of our method is from the introduced distilled auxiliary samples with ignorable training cost.

The performance on JAFFE dataset is reported in Table. 5. As noted by [16], there is a high bias in this extremely small dataset, which has only 213 images. Due to this bias, the cross-dataset evaluation on JAFFE is comparatively lower than that on CK+. However, our method still outperforms [16].

As shown in Table. 6, for MMI dataset, our method achieves comparable accuracy with [16] with few computation cost, outperforms the baseline by a large margin, which is from 60.82% to 63.34%.

We also conduct a cross-dataset evaluation on FER-2013. FER-2013 is constructed for challenges and has huge variations introduced by expressive ways, head poses, scales, and etc. Due to the heavy variations existed in FER-2013, the performance under the cross-dataset setting is inferior to that on CK+. In this challenging case, our method still achieves a similar accuracy with [16] with seven distilled auxiliary samples.

4.4.3 Visualization of Selected Samples

We visualize selected auxiliary examples from MS1M in Figure. 3, and the distilled auxiliary samples in Figure. 4. In total, our method selects 117, 369 auxiliary samples from MS1M.



Fig. 3. Visualization of the selected auxiliary samples from MS1M database based on RAF-DB. Each row corresponds to one expression. The confidences of images in the same row are decreasing. Best viewed in color.

TABLE 1
Inner-dataset comparison of our method with previous works on RAF-DB. VAS stands for vanilla auxiliary samples, DAS stands for distilled auxiliary samples.

Method	Accuracy (%)
FSN [63]	81.10
MRE-CNN [64]	82.63
baseDCNN [58]	82.66
DLP-CNN [58]	82.84
Center Loss [58]	82.86
PAT-VGG-F-(gender,race) [46]	83.83
PAT-ResNet-(gender,race) [46]	84.19
VGG-F (baseline)	85.15
ResNet-34 (baseline)	84.63
VAS + VGG-F	85.84
VAS + ResNet-34	85.84
DAS + VGG-F	86.55
DAS + ResNet-34	85.24

Each row of Figure. 3 corresponds to one facial expressions. The images in each row are sorted by the distance between their feature and the nearest class centroid. Although there are large variations in MS1M, and a large domain gap between MS1M and the anchor dataset (RAF-DB), we can observe that the auxiliary samples selected are still highly related to activated facial expression. From the images shown in Figure. 3, despite there are heavy illumination changes (the first column, second row), large poses (the first column and third column, sixth row), occlusions (fourth column, first row), our method still assigns correct expression labels for those samples. The high quality of those selected samples can explain why our method achieves a better performance after utilizing those auxiliary

TABLE 2
Inner-dataset comparison of our method with previous works on FER-2013. The performance of previous works are cited from [65].

Method	Accuracy (%)
ECNN [66]	69.96
DLSVM. [67]	71.2
Ron et al [68]	72.1
PAT-VGG-F-(gender,race). [46]	72.16
PAT-ResNet-(gender,race). [46]	72.00
VGG-F (baseline)	71.79
ResNet-34 (baseline)	70.89
VAS + VGG-F	72.08
VAS + ResNet-34	70.98
DAS + VGG-F	73.27
DAS + ResNet-34	71.20

TABLE 3
Inner-dataset comparison of our method with previous works on CK+.
The performance of previous works are cited from [46].

Method	Accuracy (%)
Inception [21]	93.20
PAT-VGG-F-(gender,race) [46]	95.58
VGG-F (baseline) [46]	93.42
DAS + VGG-F	95.35

data.

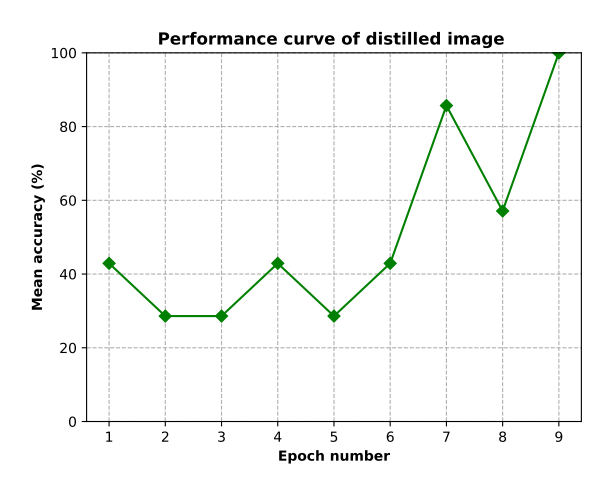


Fig. 5. Prediction curve of test set in distilled auxiliary samples. RAF-DB as the anchor dataset.

4.5 Discussion

Do the distilled auxiliary samples really contain underlying patterns? Based on the visualizations in Figure. 4, it is difficult to find any semantic meaning in them. All of the distilled images are full of specific texture patterns. This observation arouses us the question that whether those distilled images can provide useful knowledge for us. We conduct a simple experiment to test whether or not there are any underlying class related patterns in those distilled images. We save the intermediate distilled images in every ten epochs, resulting in 42 distilled images (the distillation process takes six epochs, each epoch saves 7 images). We split them into a training set and testing set by a ratio of 5:1, and then feed the split training set and testing set to

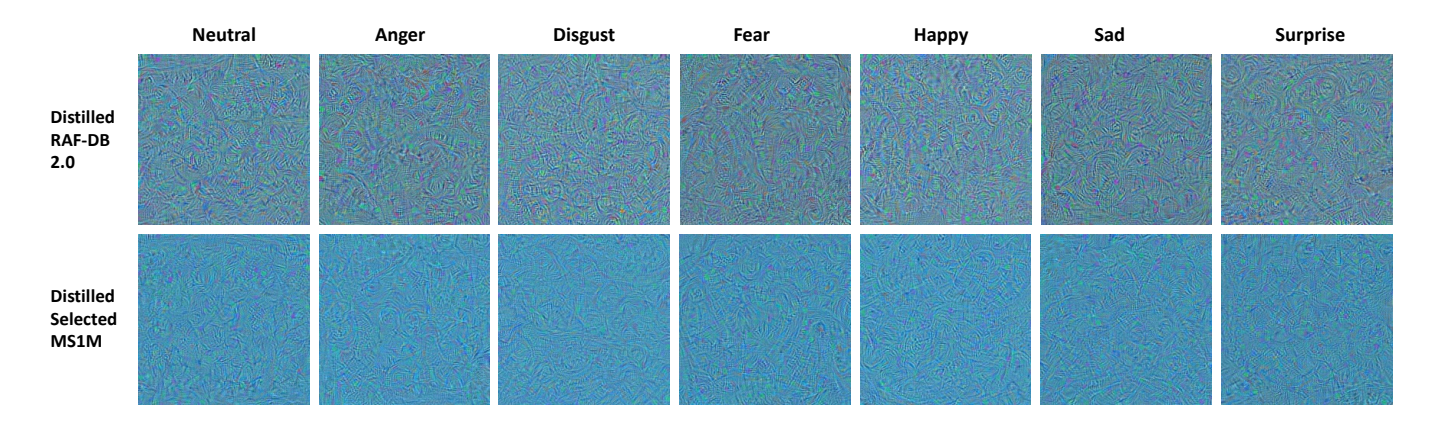


Fig. 4. Visualization of the distilled images from RAF-DB training set, and distilled images from selected samples in MS1M database. Best viewed in color.

TABLE 4
Cross-dataset comparison on CK+ dataset. DA denotes domain adaptation.

Method	Source	Target	Accuracy (%)
VGG-F+DA [16]	RAF-DB	CK+	78.00
VGG-F	RAF-DB+DAS	CK+	79.33

TABLE 5
Cross-dataset comparison on JAFFE dataset.

Method	Source	Target	Accuracy (%)
VGG-F+DA [16]	RAF-DB	JAFFE	54.26
VGG-F	RAF-DB+DAS	JAFFE	54.93

train a CNN. Our intuition is this: if those distilled auxiliary samples do not have any regular patterns corresponding to classes, then the CNN can not learn anything from them. What we observe is shown in Figure. 5. From this figure, we can find that the CNN trained on the distilled auxiliary samples converges very fast. The CNN can easily predict the images in the test set correctly, which indicates the existence of underlying patterns corresponding to different classes in each distilled sample.

5 Conclusion

In this article, we propose a simple yet effective omnisupervised baseline for facial expression recognition. Unlike previous works using unlabeled data for pretraining, we exploit and distill the useful knowledge from a large-scale unlabeled data set constructed by our method, and enhance the FER performance. We have demonstrated that the distilled knowledge from the constructed large-scale unlabeled data has high generality by achieving significant advancement in inner-dataset and cross-dataset evaluations. In the future, we will explore how to make our proposed method to collaborate the latest FER works such as PASM [10], improving the network performance from different aspects.

TABLE 6
Cross-dataset comparison on MMI dataset.

Method	Source	Target	Accuracy (%)
VGG-F+DA [16]	RAF-DB	MMI	64.13
VGG-F (baseline)	RAF-DB	MMI	60.82
VGG-F	RAF-DB+DAS	MMI	63.34

TABLE 7
Cross-dataset comparison on FER-2013 dataset.

Method	Source	Target	Accuracy (%)
VGG-F+DA [16]	RAF-DB	FER-2013	55.38
VGG-F	RAF-DB+DAS	FER-2013	55.17

REFERENCES

- [1] Y. Guo, L. Zhang, Y. Hu, X. He, and J. Gao, "Ms-celeb-1m: A dataset and benchmark for large-scale face recognition," in *European Conference on Computer Vision (ECCV)*, 2016.
- [2] P. Lucey, J. F. Cohn, T. Kanade, J. Saragih, Z. Ambadar, and I. Matthews, "The extended cohn-kanade dataset (ck+): A complete dataset for action unit and emotion-specified expression," in IEEE Conference on Computer Vision and Pattern Recognition (CVPR) Workshop, 2010.
- [3] H. Lai, P. Yan, X. Shu, Y. Wei, and S. Yan, "Instance-aware hashing for multi-label image retrieval," *IEEE Transactions on Image Processing*, 2016.
- [4] X. Zhang, Y. Wei, Z. Li, C. Yan, and Y. Yang, "Rich embedding features for one-shot semantic segmentation," IEEE Transactions on Neural Networks and Learning Systems, 2021.
- [5] H. Fan, P. Liu, M. Xu, and Y. Yang, "Unsupervised visual representation learning via dual-level progressive similar instance selection," *IEEE Transactions on Cybernetics*, 2021.
- [6] Z. Meng, P. Liu, J. Cai, S. Han, and Y. Tong, "Identity-aware convolutional neural network for facial expression recognition," in *International Conference on Automatic Face and Gesture Recognition* (FG), 2017.
- [7] F. Zhang, T. Zhang, Q. Mao, and C. Xu, "Joint pose and expression modeling for facial expression recognition," in *IEEE Conference on Computer Vision and Pattern Recognition (CVPR)*, 2018.
- [8] H. Yang, U. Ciftci, and L. Yin, "Facial expression recognition by de-expression residue learning," in IEEE Conference on Computer Vision and Pattern Recognition (CVPR), 2018.
- [9] D. Liu, N. Bellotto, and S. Yue, "Deep spiking neural network for video-based disguise face recognition based on dynamic facial movements," *IEEE Transactions on Neural Networks and Learning* Systems, 2020.
- [10] P. Liu, Y. Lin, Z. Meng, L. Lu, W. Deng, J. T. Zhou, and Y. Yang, "Point adversarial self-mining: A simple method for facial expression recognition," *IEEE Transactions on Cybernetics*, 2021.
- [11] Y. Zhang, X. Yu, X. Lu, and P. Liu, "Pro-uigan: Progressive face hallucination from occluded thumbnails," *arXiv preprint arXiv:2108.00602*, 2021.

TABLE 8

Computation cost of without introducing auxiliary samples, with vanilla auxiliary samples, with distilled auxiliary samples.

Method	w/o AS	w/ VAS	w/ DAS
Seconds per epoch	155	1625	156

- [12] Y. Zhang, I. W. Tsang, J. Li, P. Liu, X. Lu, and X. Yu, "Face hallucination with finishing touches," IEEE Transactions on Image Processing, 2021.
- [13] Y. Yan, F. Nie, W. Li, C. Gao, Y. Yang, and D. Xu, "Image classification by cross-media active learning with privileged information," IEEE Transactions on Multimedia, 2016.
- [14] M. R. Santander, J. H. Albarracín, and A. R. Rivera, "On the pitfalls of learning with limited data: A facial expression recognition case study," arXiv preprint arXiv:2104.02653, 2021.
- [15] F. Ma, Y. Wu, X. Yu, and Y. Yang, "Learning with noisy labels via self-reweighting from class centroids," IEEE Transactions on Neural Networks and Learning Systems, 2021.
 [16] S. Li and W. Deng, "A Deeper Look at Facial Expression Dataset
- Bias," IEEE Transactions on Affective Computing, 2020.
- [17] D. Erhan, A. Courville, Y. Bengio, and P. Vincent, "Why does
- unsupervised pre-training help deep learning?" in *ICML*, 2010. X. Wang, R. Zhang, C. Shen, T. Kong, and L. Li, "Dense contrastive learning for self-supervised visual pre-training," in CVPR, 2021.
- [19] T. Wang, J.-Y. Zhu, A. Torralba, and A. A. Efros, "Dataset distillation," arXiv preprint arXiv:1811.10959, 2018.
- [20] P. Liu, S. Han, Z. Meng, and Y. Tong, "Facial expression recognition via a boosted deep belief network," in IEEE Conference on Computer Vision and Pattern Recognition (CVPR), 2014.
- [21] A. Mollahosseini, D. Chan, and M. H. Mahoor, "Going deeper in facial expression recognition using deep neural networks," in IEEE Winter Conference on Applications of Computer Vision (WACV), 2016.
- [22] Y. Li, J. Zeng, S. Shan, and X. Chen, "Occlusion aware facial expression recognition using cnn with attention mechanism," IEEE Transactions on Image Processing, 2018.
- [23] Z. Zhang, M. Lyons, M. Schuster, and S. Akamatsu, "Comparison between geometry-based and gabor-wavelets-based facial expression recognition using multi-layer perceptron," in International Conference on Automatic Face and Gesture Recognition (FG), 1998.
- [24] Y. Zhang and Q. Ji, "Active and dynamic information fusion for facial expression understanding from image sequences," IEEE Transactions on Pattern Analysis and Machine Intelligence, 2005.
- [25] Y.-l. Tian, T. Kanade, and J. F. Cohn, "Evaluation of gabor-waveletbased facial action unit recognition in image sequences of increasing complexity," in International Conference on Automatic Face and Gesture Recognition (FG), 2002.
- [26] M. Eckhardt, I. Fasel, and J. Movellan, "Towards practical facial feature detection," International Journal of Pattern Recognition and Artificial Intelligence, 2009.
- [27] P. Yang, Q. Liu, and D. N. Metaxas, "Boosting coded dynamic features for facial action units and facial expression recognition," in IEEE Conference on Computer Vision and Pattern Recognition (CVPR), 2007.
- [28] Y. Hu, Z. Zeng, L. Yin, X. Wei, X. Zhou, and T. S. Huang, "Multiview facial expression recognition," in International Conference on Automatic Face and Gesture Recognition (FG), 2008.
- [29] M. Dahmane and J. Meunier, "Emotion recognition using dynamic grid-based hog features," in International Conference on Automatic Face and Gesture Recognition (FG), 2011.
- [30] T. Senechal, V. Rapp, H. Salam, R. Seguier, K. Bailly, and L. Prevost, 'Combining aam coefficients with lgbp histograms in the multikernel svm framework to detect facial action units," in International Conference on Automatic Face and Gesture Recognition (FG), 2011.
- [31] M. F. Valstar, M. Mehu, B. Jiang, M. Pantic, and K. Scherer, "Metaanalysis of the first facial expression recognition challenge," IEEE Transactions on Systems, Man, and Cybernetics, Part B (Cybernetics),
- [32] S. Zafeiriou and M. Petrou, "Sparse representations for facial expressions recognition via 1 1 optimization," in IEEE Conference on Computer Vision and Pattern Recognition (CVPR) Workshop, 2010.
- [33] Z.-L. Ying, Z.-W. Wang, and M.-W. Huang, "Facial expression recognition based on fusion of sparse representation," in International Conference on Intelligent Computing, 2010.

- [34] P. Liu, S. Han, and Y. Tong, "Improving facial expression analysis using histograms of log-transformed nonnegative sparse representation with a spatial pyramid structure," in *International Conference* on Automatic Face and Gesture Recognition (FG), 2013.
- [35] L. Zhong, Q. Liu, P. Yang, B. Liu, J. Huang, and D. N. Metaxas, 'Learning active facial patches for expression analysis," in IEEE Conference on Computer Vision and Pattern Recognition (CVPR), 2012.
- [36] X. Xiang and T. D. Tran, "Linear disentangled representation learning for facial actions," IEEE Transactions on Circuits and Systems for Video Technology, 2018.
- [37] S. Dai and H. Man, "Mixture statistic metric learning for robust human action and expression recognition," IEEE Transactions on Circuits and Systems for Video Technology, 2018.
- S. Xie, H. Hu, and Y. Chen, "Facial expression recognition with two-branch disentangled generative adversarial network," IEEE Transactions on Circuits and Systems for Video Technology, 2020.
- [39] B. Pan, S. Wang, and B. Xia, "Occluded facial expression recognition enhanced through privileged information," in ACM International Conference on Multimedia (MM), 2019.
- [40] L. Shan and D. Weihong, "Deep Facial expression recognition: A survey," IEEE Transactions on Affective Computing, 2020.
- X. J. Zhu, "Semi-supervised learning literature survey," Tech. Rep., 2005.
- [42] A. Tarvainen and H. Valpola, "Mean teachers are better role models: Weight-averaged consistency targets improve semi-supervised deep learning results," in Annual Conference on Neural Information Processing Systems (NeurIPS), 2017.
- [43] S. Laine and T. Aila, "Temporal ensembling for semi-supervised learning," in International Conference on Learning Representations (ICLR), 2017.
- [44] Y. Luo, R. Ji, T. Guan, J. Yu, P. Liu, and Y. Yang, "Every node counts: Self-ensembling graph convolutional networks for semisupervised learning," Pattern Recognition, 2020.
- [45] I. Radosavovic, P. Dollár, R. Girshick, G. Gkioxari, and K. He, "Data distillation: Towards omni-supervised learning," in IEEE Conference on Computer Vision and Pattern Recognition (CVPR), 2018.
- [46] J. Cai, Z. Meng, A. S. Khan, Z. Li, J. O'Reilly, and Y. Tong, "Probabilistic attribute tree in convolutional neural networks for facial expression recognition," arXiv preprint arXiv:1812.07067, 2018.
- [47] R. Johnson and T. Zhang, "Accelerating stochastic gradient descent using predictive variance reduction," in Advances in Neural Information Processing Systems (NeurIPS), 2013.
- Y. Luo, L. Zheng, T. Guan, J. Yu, and Y. Yang, "Taking a closer look at domain shift: Category-level adversaries for semantics consistent domain adaptation," in IEEE Conference on Computer Vision and Pattern Recognition (CVPR), 2019.
- [49] Q. Zhang, J. Zhang, W. Liu, and D. Tao, "Category anchorguided unsupervised domain adaptation for semantic segmentation," in Annual Conference on Neural Information Processing Systems (NeurIPS), 2019.
- [50] S. Li and W. Deng, "Reliable crowdsourcing and deep localitypreserving learning for unconstrained facial expression recognition," IEEE Transactions on Image Processing, 2018.
- I. J. Goodfellow, D. Erhan, P. L. Carrier, A. Courville, M. Mirza, B. Hamner, W. Cukierski, Y. Tang, D. Thaler, D.-H. Lee *et al.*, "Challenges in representation learning: A report on three machine learning contests," Neural Networks, 2015.
- [52] M. J. Lyons, S. Akamatsu, M. Kamachi, J. Gyoba, and J. Budynek, "The japanese female facial expression (jaffe) database," in International Conference on Automatic Face and Gesture Recognition (FG),
- [53] M. Pantic, M. Valstar, R. Rademaker, and L. Maat, "Web-based database for facial expression analysis," in IEEE International Conference on Multimedia and Expo (ICME), 2005.
- [54] K. Zhang, Z. Zhang, Z. Li, and Y. Qiao, "Joint face detection and alignment using multitask cascaded convolutional networks," IEEE Signal Processing Letters, 2016.
- [55] O. M. Parkhi, A. Vedaldi, and A. Zisserman, "Deep face recognition," in British Machine Vision Conference (BMVC), 2015.
- K. He, X. Zhang, S. Ren, and J. Sun, "Deep residual learning for image recognition," in IEEE Conference on Computer Vision and Pattern Recognition (CVPR), 2016.
- [57] A. Paszke, S. Gross, F. Massa, A. Lerer, J. Bradbury, G. Chanan, T. Killeen, Z. Lin, N. Gimelshein, L. Antiga, A. Desmaison, A. Kopf, E. Yang, Z. DeVito, M. Raison, A. Tejani, S. Chilamkurthy, B. Steiner, L. Fang, J. Bai, and S. Chintala, "Pytorch: An imperative

- style, high-performance deep learning library," in Annual Conference on Neural Information Processing Systems (NeurIPS), 2019.
- [58] S. Li, W. Deng, and J. Du, "Reliable crowdsourcing and deep locality-preserving learning for expression recognition in the wild," in *IEEE Conference on Computer Vision and Pattern Recognition* (CVPR), 2017.
- [59] Y. Luo, P. Liu, T. Guan, J. Yu, and Y. Yang, "Significance-aware information bottleneck for domain adaptive semantic segmentation," in *International Conference on Computer Vision (ICCV)*, 2019.
- [60] —, "Adversarial style mining for one-shot unsupervised domain adaptation," in *NeurIPS*, 2020.
- [61] Y. Luo, P. Liu, L. Zheng, T. Guan, J. Yu, and Y. Yang, "Category-level adversarial adaptation for semantic segmentation using purified features," *IEEE Transactions on Pattern Analysis and Machine Intelligence*, 2021.
- [62] G. Tjio, P. Liu, J. T. Zhou, and R. S. M. Goh, "Adversarial semantic hallucination for domain generalized semantic segmentation," in WACV, 2021.
- [63] S. Zhao, H. Cai, H. Liu, J. Zhang, and S. Chen, "Feature selection mechanism in cnns for facial expression recognition." in *British Machine Vision Conference (BMVC)*, 2018.
- [64] Y. Fan, J. C. Lam, and V. O. Li, "Multi-region ensemble convolutional neural network for facial expression recognition," in International Conference on Artificial Neural Networks (ICANN), 2018.
- [65] J. Cai, "Improving person-independent facial expression recognition using deep learning," *Ph.D. Thesis*, 2019.
 [66] G. Wen, Z. Hou, H. Li, D. Li, L. Jiang, and E. Xun, "Ensemble
- [66] G. Wen, Z. Hou, H. Li, D. Li, L. Jiang, and E. Xun, "Ensemble of deep neural networks with probability-based fusion for facial expression recognition," Cognitive Computation, 2017.
- [67] Y. Tang, "Deep learning using linear support vector machines," in International Conference on Machine Learning (ICML) Workshop, 2013.
- [68] R. Breuer and K. Kimmel, "A deep learning perspective on the origin of facial expressions," Master Thesis, 2017.